

BEAMS IN PLASMA

Source of an Annular Controlled-Radius Plasma for a Plasma Relativistic Microwave Oscillator

O. T. Loza, A. V. Ponomarev, P. S. Strelkov, D. K. Ul'yanov, and A. G. Shkvarunets

Institute of General Physics, Russian Academy of Sciences, ul. Vavilova 38, Moscow, 117942 Russia

Received June 21, 1996; in final form, July 26, 1996

Abstract—A technique of a plasma production for the relativistic plasma microwave generator is described. This technique permits the density and radius of the annular plasma in each shot to be controlled. The results of measurements of the plasma parameters are presented, and the physical processes occurring in the plasma source are discussed.

1. INTRODUCTION

Experimental studies in relativistic plasma microwave electronics were carried out from 1982 [1] until recently [2]. Over this time, significant attention was paid to the development of plasma sources and investigations of properties of the produced plasma. The results of our work in this direction are described in the present paper.

The operation of a plasma microwave oscillator is based on the effect of the Cherenkov interaction of a high-current relativistic electron beam (REB) with a slow eigenmode of a plasma waveguide. Slow waves with phase velocities lower than the speed of light exist in any plasma waveguide placed in the magnetic field. For this reason, it seems that any plasma source can be used in studies of microwave oscillators based on REB–plasma interaction. However, there are two basic experimental requirements: the arrangement of the experiment should be simple, and the efficiency of conversion of the REB energy into the electromagnetic radiation should be high. To meet these requirements, we designed a special plasma source.

It is obvious that the problem of the electron beam–plasma interaction is simplest if a plasma is placed inside a cylindrical metal waveguide with smooth walls and the plasma column is uniform over its length and azimuth. In order to study only the Cherenkov interaction and exclude the cyclotron effects, we should place the plasma into a longitudinal magnetic field so that the following inequality is satisfied: $\omega_{Be} \gg \omega_{pe}$, where ω_{Be} is the electron cyclotron frequency and ω_{pe} is the plasma frequency. Simple estimates show that, for the generation of the microwave radiation in the centimeter wavelength range, plasma with a density of 10^{12} – 10^{14} cm $^{-3}$ is needed. Since we study only high-frequency electron oscillations, ion parameters are unimportant. It is necessary that the plasma be collisionless, i.e., $\omega_{pe} \gg \omega \gg \nu_{ei}$, ν_{e0} , where ω is the frequency of the excited oscillations, and ν_{ei} , ν_{e0} are the frequencies of

electron–ion and electron–neutral collisions. This condition is easily satisfied in the experiment. Finally, in the simplest statement of the problem, the electron beam is assumed to be uniform over radius.

However, the latter condition (i.e., the beam uniformity in the radial direction) cannot be satisfied in the experimental microwave generator for the two following reasons. First, there should be a gap between the beam and plasma in the radial direction; i.e., their cross sections should not overlap. If there is no gap, the plasma, flowing along the magnetic field, arrives at the diode of the high-current electron accelerator and causes the breakdown in the diode. A thin metal foil separating the diode from the plasma waveguide does not produce a desirable effect, because the foil of ≥ 10 μ m thickness causes a large spread of beam electrons ($E_e \sim 500$ eV) in angles, which strongly decreases the efficiency of the Cherenkov interaction [3]. It follows that the plasma column should be hollow (with annular cross section). The relativistic beam is usually injected inside this plasma tube (Fig. 1). Since the REB source with the plasma waveguide must be protected from the action of the plasma, we should arrange a gap between the beam and the plasma. To provide a matching of the plasma waveguide with the vacuum radiating waveguide, we should have another gap between the plasma and the wall of the metal waveguide. Figure 1 shows the schematic of the plasma microwave oscilla-

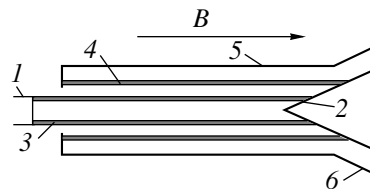


Fig. 1. Schematic of the relativistic microwave oscillator: (1) accelerator cathode, (2) collector, (3) REB, (4) plasma, (5) metal tube, (6) coaxial radiating horn.

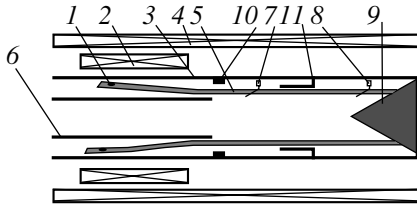


Fig. 2. Schematic of the microwave source.

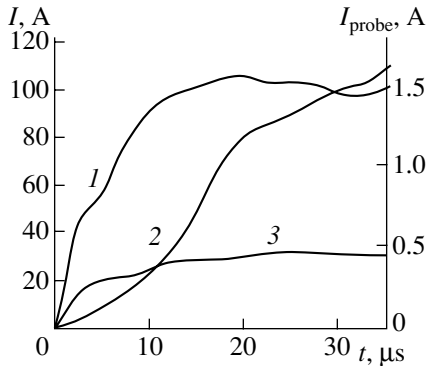


Fig. 3. Time dependences of the (1) discharge current, (2) probe current, and (3) collector current ($P = 4.5 \times 10^{-4}$ torr, $B_1 = 1.64$ T, $B_2 = 0$).

tor with the annular plasma column and the coaxial metal radiating horn. If there is a gap between the plasma and the metal waveguide wall, then the wave formed in the plasma waveguide has a high radial component of the electric field on the metal wall, and the substantial part of the microwave energy is transported in the gap between the plasma and the metal wall. Thereby, we achieve a small reflection coefficient in the transition of the wave from the plasma waveguide to the coaxial radiating horn. This allows us to reach a fair generator efficiency of $\sim 20\%$ at high output power [4].

In the present paper, we describe an annular-plasma source meeting all the requirements stated above. The only disadvantage of the experimental source is the presence of azimuthal inhomogeneities, which can disturb the plasma-wave structure. This complicates the physical picture of the process and even can make it impossible to analyze theoretically the experimental results on the microwave generation.

In the present work:

- (1) The main parameters of the annular plasma were measured experimentally;
- (2) Low-frequency plasma density oscillations were observed;
- (3) The technique for controlling the plasma radius (without changing the relativistic-beam radius) in the region of the REB-plasma interaction is described;

- (4) A physical model that describes the processes occurring in the plasma source is suggested.

2. SCHEMATIC OF THE PLASMA SOURCE

Figure 2 shows the schematic of the plasma source. A filamentary cathode 1 from the tungsten wire (0.8 mm in diameter) had a shape of a ring 21 mm in diameter. The anode was a metal chamber 3 connected to a collector 9. A solenoid 4 produced a uniform magnetic field (1.7 T) at the device axis. The plasma 5 was produced by the ionization of a gas filling the chamber (xenon at a pressure of 4.5×10^{-4} torr) by an electron beam, emitted by the thermocathode 1 and focused by a strong magnetic field. A solenoid 2 was used to control the plasma diameter. The plasma density was measured by probes 7 and 8. The amplitude of the voltage pulse applied to the cathode was 600 V; the pulse duration was $T \sim 100$ μ s. The discharge current (5–100 A) increased rapidly for 2 μ s and reached its maximum in 30 μ s. The plasma density increased for 30 μ s (Fig. 3). The plasma density was controlled by adjusting the filament current and varied in the range 10^{11} – 5×10^{13} cm^{-3} .

The efficiency of a microwave generator depends strongly on the dimension of the gap between the REB and the plasma. For this purpose, we designed a system for controlling the plasma radius without changing the radius of the plasma-source cathode.

3. CONTROLLING THE PLASMA RADIUS

The system for controlling the plasma radius (Fig. 2) is based on the use of the superposition of the main quasisteady field (solenoid 4) and the pulsed controlling field (solenoid 2). The main magnetic field, which is uniform over the system length, confines the plasma and the relativistic beam in the system. The controlling field affects only the electron beam (which produces the plasma) in the local region near the cathode 1. To prevent the relativistic beam from the action of the controlling magnetic field, the copper tube 6 is inserted between the beam and the plasma. The thickness of its wall is such that the magnetic fields are separated: the main field of 5.4 ms duration penetrates through the wall but the controlling field of 70 μ s duration does not penetrate through it. The proper magnetic fields and the coil positions were calculated numerically.

Let us analyze the operation of the described device. The plasma-source cathode (1) is in the superposed magnetic field $\mathbf{B}_\Sigma = \mathbf{B}_1 + \mathbf{B}_2$, where \mathbf{B}_1 is the main field, and \mathbf{B}_2 is the controlling field. As the distance from the cathode increases, the contribution from the controlling magnetic field decreases, and the electron beam and, consequently, the plasma produced by this beam contract. The conservation law for the magnetic flux takes the following form:

$$B_1 r_c^2 - B_2 (r_c^2 - r_t^2) = B_1 r_{pl}^2, \quad (1)$$

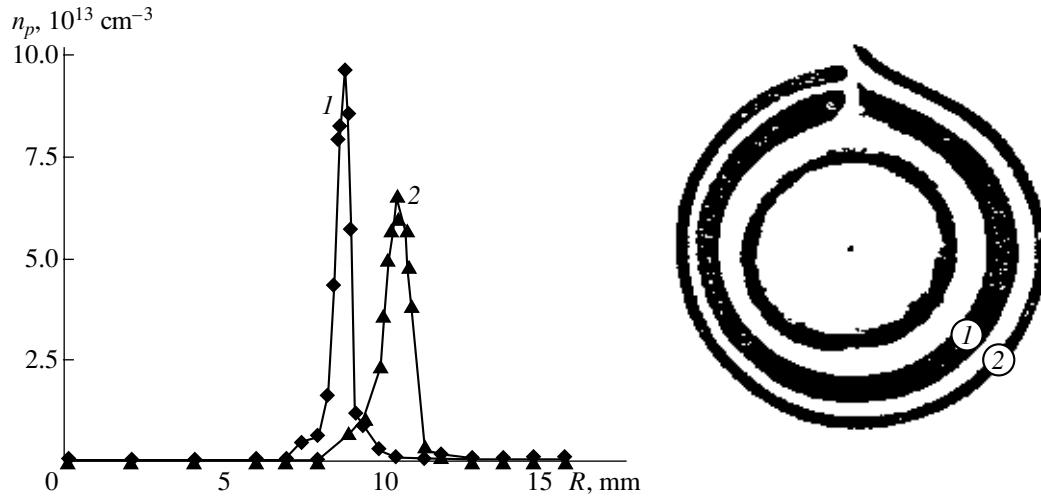


Fig. 4. Radial profile of the plasma density and the plasma imprint in the (1) presence and (2) absence of the controlling field ($B_1 = 1.64$ T, $B_2 = 1.04$ T, $I_{\text{dis}} = 80$ A, $P = 4.5 \times 10^{-4}$ torr). Imprint 1 is for a series of three shots with the different values of the controlling magnetic field: $B_2 = 1.04$; 0.82, and 0.73 T.

where r_c is the cathode radius, r_t is the outer radius of the copper tube, and r_{pl} is the plasma radius at a large distance from the controlling-field coil. For the annular plasma to have the sharp boundaries, the controlling field should be constant during the time interval between switching-on the plasma source and the REB injection. Figure 3 shows the time dependence of the discharge current and current at the probe crossing the wall of the annular plasma along radius. As is seen, the probe current reaches a value close to a maximum value during 30 μ s; i.e., this time is sufficient for producing the maximum plasma density. For this reason, the plasma source and the REB injection are switched-on, respectively, 20 and 50 μ s after switching-on the controlling field. Hence, the plasma is produced in the nearly constant magnetic field, which varies by not more than 10%.

For the cathode radius 10.5 mm, the system described makes it possible to vary the plasma radius in the range from 8 to 10.5 mm. With the main and controlling fields oriented in the same direction, it is possible to obtain plasma whose radius is larger than the cathode radius. Note that the maximum and minimum plasma radii are determined, respectively, by the input-diaphragm 10 and the outer radius of the copper tube 6 (Fig. 2).

4. MEASUREMENTS OF THE PLASMA PROFILE

Parameters of a relativistic microwave generator depend on the radial profile of the plasma density. This profile was measured with the movable Langmuir probe, whose dimensions in the radial and azimuthal directions were $\delta R = 0.2$ mm and $L_\phi = 3$ mm, respectively. We measured the electron saturation current for a probe bias of 13 V. When the bias was -13 V, the

probe detected only the electrons from the plasma cathode. It turned out that, for the bias $+13$ V, the current was about 7 times higher than for -13 V. The current was measured with a step of 0.25 mm along radius. The plasma density profiles were measured for the following parameters of the system: the controlling magnetic field was equal to 0 and 1.04 T; the main field was 1.64 T; and the discharge current was equal to 5, 20, and 80 A. The probe signal showed that the density oscillations occurred primarily at the outer plasma boundary, while they were practically absent at the axis of the annular plasma column. The time dependence of the probe current was well reproducible in the experiments, and we could measure the density profile by displacing the probe from shot to shot.

Figure 4 shows the density profiles measured at 30 μ s after switching-on the plasma-source-voltage pulse (by that time, the plasma density reaches its maximum) and "imprints" of the plasma and relativistic beam at the thermosensitive paper for a discharge current of 80 A. The profiles were reproducible if the current exceeded a certain threshold (which was 20 A for a controlling field of 1.04 T and 80 A in the absence of the controlling field). If the current was below the threshold current, we could not obtain reproducible profiles. The density increased more rapidly when the controlling field was switched on. The shape of the density profiles remained constant during the plasma creation.

Therefore, it is possible to vary the plasma density in the experiments in two ways: either by varying the discharge current or by varying the delay time between the REB injection and the plasma-source switching-on in the range from 0 to 30 μ s. In order to restore the density profiles from the probe data, the probe current was calibrated using the microwave technique described

below. It is easy to see in Fig. 4 that, with the controlling field applied, the mean radius of the annular plasma changes (from 10.5 to 8 mm), and its thickness decreases (from 0.8 to 0.6 mm).

5. PROBE MEASUREMENTS OF THE DENSITY AND TEMPERATURE OF THE PLASMA

The plasma parameters (temperature, potential, and density) were measured by the Langmuir probe crossing the plasma along radius. A bell-shaped pulse with a base duration of 15 μ s was applied to the probe. The probe signal and the voltage pulse were applied to vertical and horizontal deflector plates of an oscillograph, which, therefore, displayed the I–V characteristic of the probe. The temperature and density of the plasma were determined from the Langmuir-probe theory. The temperature was determined from the slope of the function $\ln I_{\text{probe}}(U)$.

From the probe data, for the discharge initiated at a gas pressure of 4.5×10^{-4} torr with the discharge current $I_{\text{dis}} = 25$ A, we obtained that the plasma potential was 6 V, the temperature was 3 eV, and the plasma density was 2×10^{13} cm $^{-3}$. The microwave measurements gave nearly the same plasma density.

6. MEASUREMENTS OF THE PLASMA DENSITY BY THE MICROWAVE TECHNIQUE

The absolute values of the plasma density were measured by the microwave-resonator method. We chose this method for the following reasons. First, this method allowed us to measure the plasma density without disturbing the geometry of the electrodynamic system of the relativistic plasma microwave generator. Second, for such small products of the plasma density by its thickness that were usually obtained in our system, it was difficult to use the interferometry technique.

An antenna was installed at the collector axis (9, Fig. 2). The voltage pulse was fed from the microwave generator to this antenna. The antenna excited the resonator formed by the collector and an additional

microwave reflector (11) which was placed at a distance of 19 cm from the collector. This reflector consisted of a diaphragm and a tube 2.2 cm in diameter and 5 cm in length, so that the plasma was inside this tube. The reflector was movable and could be displaced along the axis. The power that was reflected from the antenna was directed by a circulator into a detector, whose signal was led to the oscilloscope.

In the absence of a plasma, the resonator length was adjusted in such a way that there was no resonance for the E_{01m} mode. We assumed that other modes were absent in this resonator (the validity of this assumption is discussed below). In this case, all the input power was reflected from the antenna. If a plasma with the monotonically increasing density appeared in the resonator, the dispersion characteristics of the plasma waveguide varied with time. At some moment, when the plasma waveguide occurred to be in the resonance with a microwave signal, the power reflected from the antenna became minimum. Since the plasma density continued to increase, the waveguide was nonresonance again, and the reflected signal returned to its high level. Hence, in the oscillogram of the reflected signal, there were a number of sharp minima, each of them corresponding to a certain density; to derive this density, we made some assumptions, which are described below.

It should be noted that the version of the microwave-resonator method used here differed substantially from the conventional one (see, e.g., [5]). In our device, the plasma in the resonator was nonuniform: it was a thin-wall annular plasma column. A special computer program was created to calculate the dispersion characteristic of the resonator. On the other hand, because of the small thickness of the walls of the annular plasma, we could measure the supercritical plasma density up to 10^{13} cm $^{-3}$ at a frequency of 10.5 GHz. We note that radiation with the smaller wavelength could not be used, since the wavelength was restricted by the diameter of the reflector tube 11. The frequency was chosen such that this tube was a beyond-cutoff waveguide for the E_{01} mode.

To derive the plasma density from the measured signals, we made the following assumptions:

- (1) The magnetic field is infinitely strong; $\omega_{Be} \gg \omega$, ω_{pe} , where ω_{Be} is the electron gyrofrequency, ω is the microwave frequency, and ω_{pe} is the plasma frequency;
- (2) The radial profile for the plasma density is given;
- (3) Both the field and plasma in the resonator are axisymmetric;
- (4) Only the E_{01m} mode exists in the resonator;
- (5) The microwave radiation has a weak effect on the plasma.

The excitation of the only E_{01m} mode in the resonator was ensured by locating the antenna at the resonator axis, since other modes that could be excited in this geometry did not have the longitudinal component of

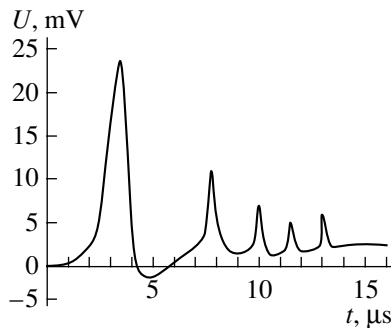


Fig. 5. Time dependence of the signal from the microwave detector ($I_{\text{dis}} = 80$ A, $P = 4.5 \times 10^{-4}$ torr, $B_1 = 1.64$ T, $B_2 = 0$).

the electric field at the resonator axis. We conducted the test measurements of the signal reflected from the antenna for different resonator lengths in the absence of a plasma. Their results showed that the amplitude of resonances for the E_{01m} mode was larger by at least two orders than that for other possible modes.

To estimate the effect of the microwave radiation on the plasma parameters, we decreased the input power by a factor of about 5. Although the amplitude of the resonant minimums diminished, neither the shape nor time positions of the minimums change. Indirectly, this indicates that the microwave radiation weakly affects the plasma parameters.

Figure 5 shows the typical time dependence of the signal reflected from the antenna (here, the inverted signal is shown in which a constant voltage of 0.4 V is filtered off). Zero time corresponds to the switching-on of the plasma source. In the figure, five pronounced resonant maximums are seen. The time positions of these maximums did not shift from shot to shot and were reproduced correct to nearly $0.2 \mu\text{s}$, which indicates to a fair reproducibility of discharges in the plasma source.

The accuracy of determining of an absolute value of the plasma density depends primarily on the accuracy of measurements of the radial profiles of the plasma density. We carried out a series of measurements of the radial density profiles to diminish the error. Based on their results, we estimate the error of the measurements of the plasma density as $\pm 20\%$.

The measurements were conducted in the absence of a controlling magnetic field. The discharge current was 80 A. The pressure was 4.5×10^{-4} torr. It turned out that a probe current of 100 mA corresponded to a plasma density of $0.5 \times 10^{13} \text{ cm}^{-3}$, and a current of 290 mA corresponded to a density of $1.5 \times 10^{13} \text{ cm}^{-3}$. Such a quasilinear dependence allowed us to recalculate the probe current to the plasma density; the electron temperature was assumed to be constant.

7. MEASUREMENTS OF DIMENSIONS OF THE PLASMA-DENSITY INHOMOGENEITIES

We observed oscillations in the signals of the probes crossing the annular plasma along radius (Fig. 6). These oscillations, which are due to the inhomogeneity of the plasma over the azimuth, hinder the creation of the efficient microwave generators. We conducted a series of experiments in order to determine the nature of the observed oscillations.

For this purpose, we used the Langmuir probes (7, 8, Fig. 2). After the alignment of the plasma source, the probes were positioned at the same angle φ at a distance L from each other along the z -axis. In the experiments, the xenon pressure was 4.5×10^{-4} torr, and the plasma density was $n_p \approx 2 \times 10^{13} \text{ cm}^{-3}$. The probe current was measured at various probe positions: the angle

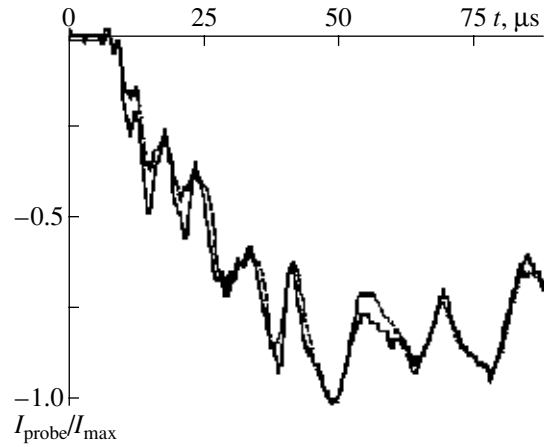


Fig. 6. Signals from the Langmuir probes ($\Delta\varphi = +10^\circ$, $L = 30 \text{ mm}$, $\Delta T = 0$).

between the probes was varied from 0° to 30° with a step of 5° clockwise and counter-clockwise, and the distance between them was $L = 10, 30, 50, 70$, and 100 mm . 10° corresponded to a displacement by a 1.25 mm distance at the outer wall of the annular plasma.

It turned out that the oscillations in the signals of the two probes are very similar. In addition, the time delay was observed in the oscillations between these two probes. To determine the delay time, we used the correlation analysis.

We used the following procedure: in each oscillogram, we found a number of times corresponding to the extremums of the signal derivative, t_j . Further, we constructed the following function:

$$F(t) = \begin{cases} -1, & \text{if } [t_i; t_{i+1}] \rightarrow \min \\ +1, & \text{if } [t_i; t_{i+1}] \rightarrow \max \\ 0, & \text{if there is } [t_i; t_{i+1}] \text{ no max or min.} \end{cases}$$

Then, we determined the delay time T_{opt} , for which the correlation coefficient

$$R(T) = \frac{\int F_1(t) F_2(t-T) dt}{[\int F_1^2(t) dt \int F_2^2(t) dt]^{1/2}} \quad (2)$$

is maximum. Figure 7 shows the delay time T_{opt} as a function of the angle φ for two distances $L = 1$ and 7 cm . In this case, the correlation coefficient was in the range from 0.9 to 0.95. As is seen, T_{opt} decreases monotonically as the angle φ between the probes increases. From this dependence, we can find the drift velocity of the inhomogeneities of the plasma density: $V_\varphi \approx L_\varphi / \Delta T_{\text{opt}} \approx 4 \times 10^4 \text{ cm/s}$, where L_φ is the distance between the probes in the azimuthal direction, and ΔT_{opt} is the corresponding difference between delay times (Fig. 7).

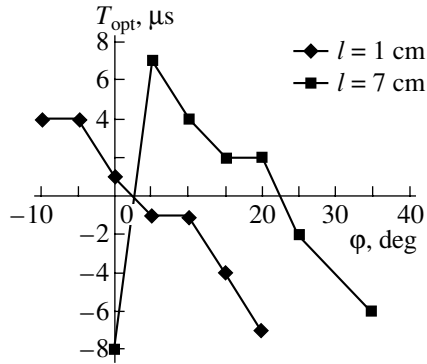


Fig. 7. Time shift T_{opt} as a function of the angle between the probes ($B_1 = 1.64$ T, $I_{\text{dis}} = 25$ A).

The radial dimension of the inhomogeneities of the plasma density can be found from Fig. 6. One can see in this figure that the period of the probe-current oscillations is about $10 \mu\text{s}$; consequently, this dimension is $\lambda_\phi = 2\pi/k_\phi = 4 \times 10^4 \times 10^{-5} \text{ cm} = 0.4 \text{ cm}$. Since, in two different curves, $T_{\text{opt}} = 0$ corresponds to the different $\Delta\phi^*$ (for $L = 1 \text{ cm}$, $\Delta\phi^* = 2^\circ$ and, for $L = 7 \text{ cm}$, $\Delta\phi^* = 22^\circ$), it follows that the density perturbations are the helical enhanced-density structures inclined at an angle of $\sim 2^\circ$ with respect to the z -axis. Hence, we obtain $k_z \approx 0.7 \text{ cm}^{-1}$. Since we can observe oscillations even if the probe crosses the entire wall of the annular plasma column, it follows that the radial dimension of inhomogeneities of the plasma density is larger or on the order of $\Delta r_p \approx 0.1 \text{ cm}$.

8. DISCUSSION OF THE EXPERIMENTAL RESULTS

In this section, we estimate roughly the rate of the plasma-density growth and suggest the possible explanations of the discrepancy between the neutral density ($1.6 \times 10^{13} \text{ cm}^{-3}$) and the electron density ($\sim 10^{14} \text{ cm}^{-3}$). We also analyze the nature of the plasma-density oscillations.

The Rate of The Plasma-Density Growth

The gas is ionized via collisions between the electrons emitted from the plasma-source cathode and neutrals as well as by high-frequency fields that arise as a result of the onset of the plasma-beam instability. The rates of both processes depend on the electron-beam current. First of all, when we estimate the rate of the plasma-density growth, we should take into account that the electrons move in both directions along the magnetic field lines (Fig. 1), because, for the electrons with energies of 600 eV, the Larmor radius is equal to $5 \times 10^{-3} \text{ cm}$. Only a portion of the total flow of electrons (approximately 1/3) moves toward the collector

and produces the plasma under investigation. For a discharge current of 95 A, a current of only 30 A was measured at the collector.

The exact time dependence of the rate of the plasma-density growth can be obtained only if we know the time dependence of the beam current, which, in turn, depends on the plasma density. Initially, a plasma is absent, and the electron current toward the collector is restricted by the space charge and cannot be larger than the limiting vacuum current of 0.3 A. The time of the neutralization of the electron beam is $(N_0\sigma V)^{-1} = 0.3 \mu\text{s}$, where N_0 is the neutral density, σ is the ionization cross section, and V is the electron velocity. After $0.3 \mu\text{s}$, the beam charge is neutralized, and the current can increase to the Pierce current of 1.6 A; in this case, the beam-electron density is $1.5 \times 10^{10} \text{ cm}^{-3}$. The further growth of the current at the collector is associated with the screening of the cathode by the plasma; as a consequence, the electric field is located near the cathode surface, and the current increases, although it remains limited by the electron space charge of the cathode sheath. Using the simple formula for the planar diode $j = 2.33 \times 10^{-6} U^{3/2}/d^2$, for the current 30 A (or $j = 60 \text{ A/cm}^2$), we estimate the dimension of the region in which the field is located as $d = 0.2 \text{ mm}$. Hence, this current is reached when the Debye radius becomes $\sim 0.07 \text{ mm}$. For $T_e = 3 \text{ eV}$, this occurs when $n_p = 10^{11} \text{ cm}^{-3}$. From these estimates, it follows that the discharge current can increase more rapidly than the plasma density, because it can reach its steady level at a plasma density 100 times lower than the maximum plasma density. We observe this effect qualitatively (Fig. 3): the discharge current reaches a value of $0.6I_{\text{max}}$ when the plasma density is still very small.

Taking into account the small duration of the leading front of the current pulse, we estimate the growth time for the plasma density for the plasma pressure $4.5 \times 10^{-4} \text{ torr}$ and the discharge current 30 A. In such a discharge, the electron energy distribution function takes the form of a plateau [6]. For this reason, we can estimate the electron energy as $eU/2 = 300 \text{ eV}$. In this case, the time of the electron-impact ionization is $15 \mu\text{s}$. This estimate is valid only if this time is much less than the ion loss time. As is known, in such discharges, the ion temperature is lower than the electron temperature; for this reason, we obtain $\tau > L/V_{i\text{max}} \sim 80 \mu\text{s}$. Hence, the assumption on the absence of losses is valid. In addition to the ionization of a gas by electrons emitted from the hot cathode, the gas may be ionized by the high-frequency fields arising in the plasma as a result of the onset of beam-plasma instability. The conditions for this instability are satisfied at $n_p > 1.5 \times 10^{10} \text{ cm}^{-3}$. However, apparently, this mechanism does not contribute much to the ionization, because the above estimate for the ionization time $\sim 15 \mu\text{s}$ agrees qualitatively with the experimentally observed time (Fig. 3).

Ratio between the Plasma and Gas Densities

In fig. 4, the maximum values of the plasma density are 7×10^{13} and $9 \times 10^{13} \text{ cm}^{-3}$ while the neutral density is $1.6 \times 10^{13} \text{ cm}^{-3}$. It seems that this discrepancy could be explained by the multiple ionization. The cross sections of the double and triple ionization of xenon are smaller than the cross section of the single ionization by a factor of 8 and 80, respectively. The ionization time for the single ionization is $15 \mu\text{s}$; consequently, for the double and triple ionization, these times are 120 and $1200 \mu\text{s}$, respectively. For this reason, the contribution from these mechanisms into the plasma production during $30 \mu\text{s}$ cannot be substantial. Thus, we observe the discrepancy between the plasma and neutral densities, and this effect cannot be explained by the multiple ionization.

Let us consider the effect of an "ion pump," which can explain this discrepancy. This effect is that the ions which are produced by the ionization of atoms entering the beam remain inside the beam due to the presence of the strong magnetic field. This effect can take place if the mean free path of xenon atoms during $30 \mu\text{s}$ is larger than the electron-beam thickness; in our case, this condition is fulfilled: the mean free path is 6 mm at the room temperature, and the beam thickness is $\sim 1 \text{ mm}$.

In principle, an increase in the plasma density could also be caused by the expansion of a plasma created at the collector. The measurements performed by two probes located in two points along the plasma column show that the collector plasma either is absent or moves with a velocity greater than 10^7 cm/s , which seems to be realistic. However, plasma parameters did not vary noticeably through the long series of shots; this fact indicates that the effect of the collector plasma can not be decisive.

Plasma-Density Oscillations

In our opinion, the most probable mechanism for exciting the observed plasma-density oscillations is the drift instability of a nonuniform plasma confined by a strong magnetic field [7]. In the theory of the drift instability, the oscillations occurring in an inhomogeneous plasma are analyzed and described in terms of the geometrical optics. We cannot use this theory in the analysis of the effects observed because the oscillation wavelength in the radial direction is larger than the thickness of the walls of the annular plasma column.

Under conditions when the geometrical optics cannot be used, the excitation of the surface drift waves by the Larmor currents in the thin surface layer of the semispace occupied by a plasma was studied in [7]. In a magnetized collisionless plasma, the low-frequency oscillations can be excited if

$$\omega_{Bi} \gg v_i, V_{Ti}/\Delta r_p, \quad (3)$$

where ω_{Bi} is the ion Larmor frequency, v_i is the collisional frequency, and V_{Ti} is the ion thermal velocity. Because the ion temperature was not measured experimentally, for estimate, we assume that $T_i/T_e = 0.1$; then we have $V_{Ti} \sim 10^4 \text{ cm/s}$. Substituting the experimental parameters into (3), we obtain $\omega_{Bi} = 2 \times 10^6 \text{ s}^{-1}$, $v_i = 2 \times 10^5 \text{ s}^{-1}$, and $V_{Ti}/\Delta r_p = 6 \times 10^5 \text{ s}^{-1}$. Hence, the conditions for the excitation of the low-frequency oscillations are satisfied. As was shown in [8], the drift currents flowing in the layer of a thickness equal to the ion Larmor radius ρ_i in a nonisothermal plasma with $T_e \gg T_i$ excite surface ion-sound waves propagating in the azimuthal direction. The instability should be expected in the frequency interval

$$k_z V_{Ti} \ll \omega \ll k_z V_{Te}. \quad (4)$$

For this interval, the oscillation spectrum and the growth rate of this instability were determined as

$$\omega = \pm k_\phi V_s, \quad \delta = \sqrt{\frac{\pi}{8}} \frac{\omega^2}{|k_z| V_{Te}}, \quad (5)$$

where k_ϕ and k_z are the azimuthal and longitudinal wave numbers, respectively; $V_s = \sqrt{kT_e/M}$ is the sound velocity; and V_{Te} is the thermal electron velocity. Let us estimate these quantities using the experimental parameters: $k_\phi = 16 \text{ cm}^{-1}$, $k_z \approx 0.7 \text{ cm}^{-1}$; $V_s = 1 \times 10^5 \text{ cm/s}$; $V_{Te} \approx 1 \times 10^8 \text{ cm/s}$; $\omega \approx 8 \times 10^5 \text{ s}^{-1}$. We obtain $k_z V_{Ti} \sim 4 \times 10^4 \text{ s}^{-1}$, $k_z V_{Te} \sim 3 \times 10^7 \text{ s}^{-1}$. The observed frequency falls into the interval described by inequalities (4). From (5), we obtain that the frequency of plasma-density oscillations is $\omega \approx 3 \times 10^6 \text{ s}^{-1}$, and the growth rate is $\delta \approx 5 \times 10^4 \text{ s}^{-1}$. These values do not contradict the experimental data; however, we cannot compare quantitatively the theory and the experiment. In a thin layer, the spectrum (5) is probably the same but the growth rate can increase by a factor of 2–3 due to the contribution from the drift currents from both plasma surfaces. For the more precise comparison of the experiments with the theory of drift oscillations occurring in a thin plasma layer in a strong magnetic field, it is necessary to conduct additional, both experimental and theoretical, studies.

9. CONCLUSION

The plasma source described above produces the completely ionized annular plasma with the sharp outer and inner boundaries. The plasma density is controlled in the range from 10^{11} to 10^{14} cm^{-3} . The controlling is performed by adjusting the discharge current. The radius of the annular plasma can be controlled in the range from 0.8 to 1.1 cm without changing the radius of the relativistic beam. This allows us to change the coupling between the REB and the plasma in the microwave oscillator.

The low-frequency (~ 100 kHz) plasma-density oscillations were observed, mostly, at the outer boundary of the annular plasma column. The oscillations amplitude decreases with decreasing the magnetic field; when the magnetic field is lower than 0.1 T, the oscillations disappear. These experimental results, as well as the estimates of the growth rate and frequency of these oscillations, lead us to the conclusion about the onset of the drift instability.

ACKNOWLEDGMENTS

The authors thank Professor A.A. Rukhadze for help with interpreting the experimental data.

This work was carried out on the "Plasma Relativistic Microwave Oscillator" device (registration no. 01-04) and was supported by the Russian Ministry of Science. This work was also supported in part by the International Science Foundation, grant nos. MO 3000 and MO 3300, and the Russian Foundation for Basic Research, project no. 94-02-03437.

REFERENCES

1. Kuzelev, M.V., Mukhametzyanov, M.S., Rabinovich, M.S., *et al.*, *Zh. Eksp. Teor. Fiz.*, 1982, vol. 83, no. 4, p. 1358; *Dokl. Akad. Nauk*, 1982, vol. 267, no. 4, p. 829.
2. Kuzelev, M.V., Loza, O.T., Ponomarev, A.V., *et al.*, *Zh. Eksp. Teor. Fiz.*, 1996, vol. 109, no. 6, p. 2048.
3. Kremontsov, V.I., Pabinovich, V.S., Rukhadze, A.A., *et al.*, *Zh. Eksp. Teor. Fiz.*, 1975, vol. 69, no. 4, p. 1218.
4. Shkvarunets, A.G., Rukhadze, A.A., and Strelkov, P.S., *Fiz. Plazmy*, 1994, vol. 20, p. 682 [*Sov. J. Plasma Phys.* (Engl. transl.), vol. 20, p. 613].
5. Heald, M.A. and Wharton, C.B., *Mikrovolnovaya diagnostika plazmy* (Plasma Diagnostics with Microwaves), Moscow: Atomizdat, 1968.
6. Nezlin, M.V., *Dinamika puchkov v plazme* (Dynamics of Beams in a Plasma), Moscow: Energoizdat, 1982.
7. Timofeev, A.V. and Shvilkin, B.N., *Usp. Fiz. Nauk*, 1976, vol. 118, no. 2, p. 273.
8. Aleksandrov, A.F., Bogdankevich, L.S., and Rukhadze A.A., *Osnovy elektrodinamiki plazmy* (Course of Plasma Electrodynamics), Moscow: Vysshaya Shkola, 1978, p. 285.

Translated by N. F. Larionova